MPC-6827: A Small-Molecule Inhibitor of Microtubule Formation That Is Not a Substrate for Multidrug Resistance Pumps

Shailaja Kasibhatla,[1] Vijay Baichwal,[2] Sui Xiong Cai,[1] Bruce Roth,[2] Ira Skvortsova,[3] Sergej Skvortsov,[4] Peter Lukas,[3] Nicole M. English,[1] Nilantha Sirisoma,[1] John Drewe,[1] Azra Pervin,[1] Ben Tseng,[1] Robert O. Carlson,[2] and Christopher M. Pleiman[2]

[1]Epicept Corporation, San Diego, California; [2]Myriad Pharmaceuticals, Inc., Salt Lake City, Utah; and Departments of [3]Therapeutic Radiology and Oncology and [4]Internal Medicine, Innsbruck Medical University, Innsbruck, Austria

Abstract

A novel series of 4-arylaminoquinazolines were identified from a cell-based screening assay as potent apoptosis inducers. Through structure-activity relationship studies, MPC-6827 and its close structural analogue, MPI-0441138, were discovered as proapoptotic molecules and mitotic inhibitors with potencies at low nanomolar concentrations in multiple tumor cell lines. Photoaffinity and radiolabeled analogues of MPC-6827 were found to bind a 55-kDa protein, and this binding was competed by MPC-6827, paclitaxel, and colchicine, but not vinblastine. MPC-6827 effectively inhibited the polymerization of tubulin *in vitro*, competed with colchicine binding, and disrupted the formation of microtubules in a variety of tumor cell lines, which together showed the molecular target as tubulin. Treatment of MCF-7 breast carcinoma or Jurkat leukemia cells with MPC-6827 led to pronounced G_2-M cell cycle arrest followed by apoptosis. Apoptosis, as determined by terminal deoxyribonucleotidyl transferase–mediated dUTP nick end labeling assay, was preceded by loss of mitochondrial membrane potential, cytochrome *c* translocation from mitochondria to nuclei, activation of caspase-3, and cleavage of poly(ADP-ribose) polymerase. MPC-6827 was equipotent in an *in vitro* growth inhibition assay in several cancer cell lines regardless of the expression levels of the multidrug resistance ABC transporters MDR-1 (Pgp-1), MRP-1, and BCRP-1. In B16-F1 allografts and in OVCAR-3, MIAPaCa-2, MCF-7, HT-29, MDA-MB-435, and MX-1 xenografts, statistically significant tumor growth inhibition was observed with MPC-6827. These studies show that MPC-6827 is a microtubule-disrupting agent with potent and broad-spectrum *in vitro* and *in vivo* cytotoxic activities and, therefore, MPC-6827 is a promising candidate for development as a novel therapeutic for multiple cancer types. [Cancer Res 2007;67(12):5865–71]

Introduction

Many of the chemotherapeutic agents presently in use for cancer treatment were discovered from the screening of libraries for small molecules that inhibit the growth of neoplastic cells. Subsequently, it has been determined that many of the clinically useful cytotoxic agents primarily act by inducing apoptosis in cancer cells (1–3). Apoptotic cell death is the consequence of a series of precisely regulated events that are frequently altered in tumor cells. Activation of caspases is a critical event for apoptosis induction (4, 5). The sequence of events that results in the activation of caspases has been broadly categorized into two pathways: the "extrinsic" pathway, characterized by the engagement of cell surface "death receptors" (6, 7), and the "intrinsic" mitochondrial mediated pathway, characterized by the release of cytochrome *c* from the mitochondrial intermembrane space into the cytosol (8–10). For either pathway, the ultimate activation of caspases ensures apoptosis induction.

The principal proapoptotic chemotherapeutic agents used for both childhood and adult cancers target tubulin, including the taxanes paclitaxel and docetaxel and the *Vinca* alkaloids vinblastine, vincristine, and vinorelbine. Considering the clinical success of these agents, tubulin represents one of the most highly validated cancer targets identified to date (11, 12). Tubulin targeting agents interfere with microtubule dynamics, leading to arrest of dividing cells in the G_2-M phase of the cell cycle, which eventually results in apoptotic cell death (13). However, emerging resistance to antimitotic agents has limited their ultimate effectiveness (14), leading to renewed interest in the discovery and development of new agents that are active in multidrug resistant (MDR) cells and that interact with tubulin at sites different from those of the taxanes and *Vinca* alkaloids (15). This field has exploded in the last few years, leading to the discovery of a variety of new small-molecule inhibitors, which have shown promising antitumor activity even in tumors expressing MDR phenotypes with the most advance being the macrolide epothilones (16, 17). MPC-6827 has displayed significant activity in inhibiting the growth of multiple tumor lines in athymic nude mice, which include human breast (MCF-7, MX-1, and MB-MDA-435), colon (HT-29), pancreas (MIAPaCa-2), ovarian (OVCAR-3), and mouse melanoma (B16). Here, we present a novel chemical class of compounds, represented by the lead compound MPC-6827, which inhibit tubulin polymerization, are not substrates for ABC MDR transporters *in vitro*, and display a broad spectrum of antitumor activity. Taken together, these results suggest that MPC-6827 may be effective in the treatment of multiple types of human tumors.

Materials and Methods

Chemical synthesis. MPC-6827 [*N*-(4-methoxyphenyl)-*N*,2-dimethylquinazolin-4-amine; Fig. 1*A*] was prepared via reaction of 4-chloro-2-methylquinazoline with 4-methoxy-*N*-methylaniline. MPI-0441138 [2-chloro-*N*-(4-methoxyphenyl)-*N*-methylquinazolin-4-amine; Fig. 1*A*] was prepared similarly via reaction of 2,4-dichloroquinazoline with 4-methoxy-*N*-methylaniline. The 4-azido analogue MPI-0441264 [*N*-(4-azidophenyl)-*N*,2-dimethylquinazolin-4-amine; Fig. 2*A*] was prepared via diazotization of the corresponding 4-amino analogue [*N*-(4-aminophenyl)-*N*,2-dimethylquinazolin-4-amine] followed by treatment with sodium azide. The tritiated

Requests for reprints: Christopher M. Pleiman, Myriad Pharmaceuticals, 320 Wakara Way, Salt Lake City, UT 84108. Phone: 801-584-1154; Fax: 801-883-3213; E-mail: cpleiman@myriad.com.

doi:10.1158/0008-5472.CAN-07-0127

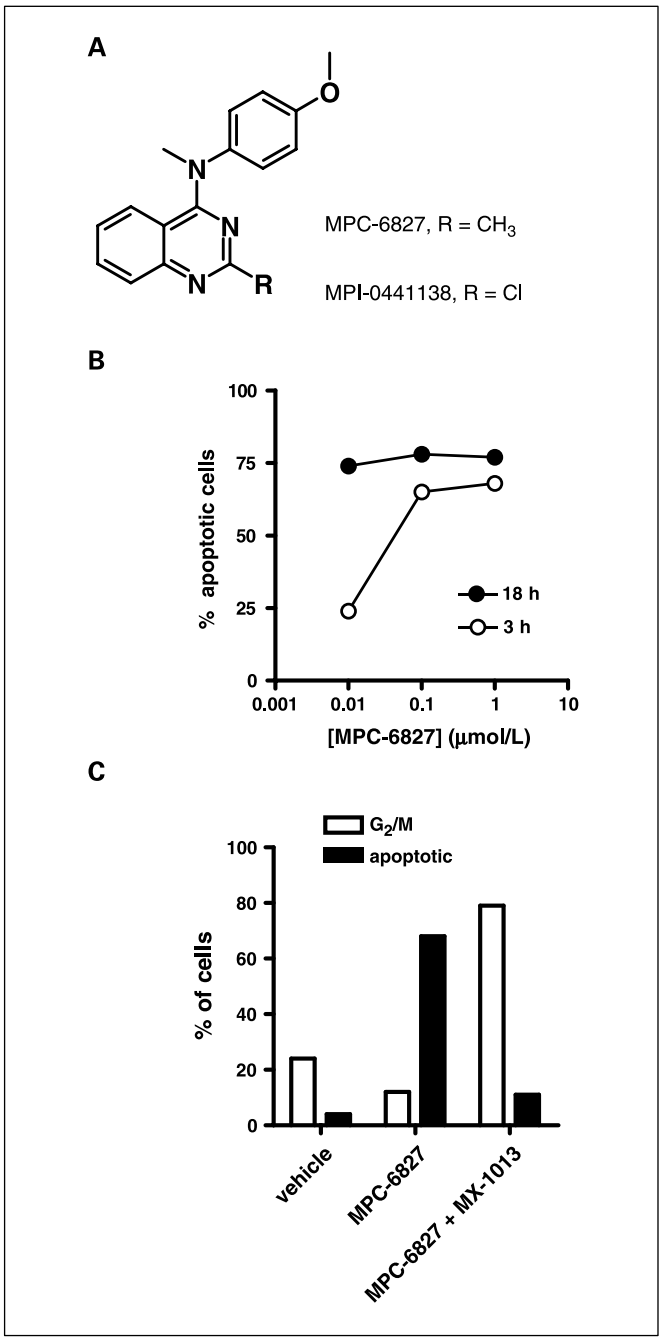

Figure 1. MPC-6827 causes rapid G_2-M mitotic arrest and apoptosis. *A,* structures of MPC-6827 and MPI-0441138. *B,* Jurkat cells were treated with the indicated concentrations of MPC-6827 for 18 h or treated for 3 h, washed, and then incubated for 18 h. Cell cycle analysis was then done to determine percent apoptosis (percent sub-G_1), which is expressed relative to cells treated with vehicle only. *C,* Jurkat cells were treated with 100 nmol/L MPC-6827 or pretreated with 10 μmol/L of a caspase inhibitor, MX-1013 (benzyloxycarbonyl-Val-Asp-fluoromethylketone), before MPC-6827 treatment and incubated for 18 h. As a control, cells were also incubated with an equivalent volume of vehicle. Representative of three independent experiments.

analogue was prepared via treatment of the corresponding 3,5-dibromo analogue [*N*-(4-amino-3,5-dibromophenyl)-*N*,2-dimethylquinazolin-4-amine] with tritium gas followed by diazotization and treatment with sodium azide ([^{3}H]MPI-0441264; Fig. 2*A*).

Cell lines and tissue culture. Jurkat, NIH-3T3, T47D, 22Rv1, Du145, A549, B16-F1, OVCAR-3, HT-29, MIAPaCa-2, MCF-7, and Caco-2 cell lines were obtained from American Type Culture Collection (ATCC) and maintained following ATCC recommendations. NCI/ADR-RES cells were obtained from National Cancer Institute (NCI; ref. 15). P388 and P388/ADR cells were obtained from NCI (18). MCF-7/VP cells (19) were obtained from Dr. Erasmus Schneider (Wadsworth Center, New York State Department of Health, Albany, NY). MCF-7/MX cells (20) were obtained from Dr. K. Cowan (University of Nebraska Medical Center, 986805 Nebraska Medical Center, Omaha, NE). NCI/ADR-RES, MCF-7/MX, P388, and P388/ADR cells were cultured in RPMI 1640 supplemented with 10% fetal bovine serum, 2 mmol/L glutaMAX, 1 mmol/L sodium pyruvate, 0.1 mmol/L nonessential amino acids, and 10 mmol/L HEPES (Invitrogen). MCF-7/VP cells were cultured in DMEM high glucose supplemented with 10% fetal bovine serum, 2.5% horse serum, 2 mmol/L glutaMAX, 1 mmol/L sodium pyruvate, 0.1 mmol/L nonessential amino acids, and 10 mmol/L HEPES. All cells were grown at 37°C in a humidified 5% CO_2 atmosphere.

Caspase activation. Cells were incubated with the test compounds in 384-well plates for 24 h. Caspase-3 fluorogenic substrate *N*-(Ac-DEVD)-*N*′-ethoxycarbonyl-R110 (21) was then added, incubated at room temperature for 3 h, and fluorescent signal resulting from caspase activation was measured using a fluorescent plate reader (Tecan Model Spectrafluor Plus). Compounds were designated as active caspase inducers if the fluorescent signal was at least 3-fold over background, based on previous demonstration that caspase-3/caspase-7 activation would yield at least this degree of fluorogenic substrate cleavage (21). Active compounds were subsequently confirmed at several concentrations to determine EC_{50} values. EC_{50} values were determined by a sigmoidal dose-response calculation (XLFit3, IDBS) and represent the concentration of compound that produces 50% the maximum observed response.

Cell cycle analysis. Human Jurkat leukemia cells were used to determine the effect of MPC-6827 on cell cycle and apoptosis. Cells were treated with various concentrations of MPC-6827 for 18 h at 37°C or treated for 3 h, washed, resuspended in growth media, and then incubated for 18 h at 37°C. In experiments done to determine the effect of caspases in cell death, cells were treated with 100 nmol/L MPC-6827 for 18 h or were pretreated with 10 μmol/L MX-1013, a pan-caspase inhibitor (21), before addition of MPC-6827. Cells were harvested at 200 × *g* and washed twice with 5 mmol/L EDTA/PBS. Cells were then resuspended in 300 μL of EDTA/PBS and 700 μL of 100% ethanol, incubated at room temperature for 1 h, and centrifuged at 200 × *g*, followed by removal of supernatant. A solution containing 100 μg/mL propidium iodide and 1 mg/mL RNase A was added to the fixed cell pellets and incubated for 1 h at room temperature. Samples were then analyzed on a flow cytometer. Flow cytometric cell cycle determinations were done on FACScalibur and data output was analyzed using Cell Quest software (Becton Dickinson).

Identification of a cellular target for MPC-6827. Jurkat cells at 1×10^7/mL in RPMI/10% fetal bovine serum were treated with vehicle, 1 μmol/L MPC-6827, 1 or 10 μmol/L colchicine, 1 or 10 μmol/L vinblastine, or 1 or 10 μmol/L paclitaxel for 1 h at 37°C, and then incubated with 100 nmol/L [^{3}H]MPI-0441264 (16.7 μmol/L, 60 Ci/mmol, and 1 mCi/mL, from American Radiolabeled Chemicals, Inc.) for 3 h at 37°C. Covalent cross-linking of [^{3}H]MPI-0441264 was achieved by exposing cells to a short-wave UV source (254 nm) for 2 or 10 min at a distance of 3.5 cm. Cells were washed twice with PBS and lysed in 200 μL of 1× radioimmunoprecipitation assay buffer [0.05 mol/L Tris-HCl (pH 7.4), 0.15 mol/L NaCl, 0.25% deoxycholic acid, 1% NP40, 1 mmol/L EDTA] plus 0.2 μL of protease inhibitor cocktail for 30 min on ice. Lysates were then spun in a microcentrifuge for 10 min at maximum speed to remove nuclei. The supernatant was transferred to a new tube containing 200 μL of 2× Tris-glycine SDS reducing sample buffer. The samples were then boiled for 5 min, and 10 μL of the boiled samples were loaded onto a 4% to 12% Tris-glycine SDS gel. The gel was subsequently stained with 1% Coomassie brilliant blue in 40% methanol/7.5% acetic acid for 2 h and then destained in several changes of 40% methanol/7.5% acetic acid. The gel was then incubated in Amplify (GE Healthcare) for 30 min at room temperature and then dried on Whatman filter paper with a gel dryer at 80°C for 2 h. The dried gel was put on Hyperfilm (GE Healthcare) in a film cassette for development at −80°C for 5 days.

***In vitro* tubulin polymerization assay.** MPC-6827 was assayed at 0.5, 5, or 50 μmol/L for effect on tubulin polymerization according to the recommended procedure of the manufacturer (Cytoskeleton, #ML113, 1 mg, MAP-rich). To 1 μL of each 100× stock of experimental compound in a 96-well plate was added 99 μL of supplemented tubulin supernatant. Incubation was carried out at 37°C in a Molecular Devices plate reader, with absorbance readings at 340 nm every minute for 1 h. The IC_{50} was the concentration found to decrease the initial rate of tubulin polymerization by 50% as calculated using Prism 3.0 software (GraphPad).

Cellular tubulin staining. A549 cells were grown overnight on 18 × 18 mm coverslips. MPC-6827 was then added at a final concentration of 10 nmol/L for 1 or 3 h at 37°C. Coverslips were removed from media and fixed in 3.7% paraformaldehyde in RPMI 1640 for 15 min at 37°C, washed thrice in 1× HBSS, and permeabilized with 0.1% Triton-X 100. Following three washes in 1× HBSS, coverslips were blocked with 1× HBSS containing 1% bovine serum albumin and 0.1% Tween 20 (blocking solution) for 1 h at room temperature. Blocked coverslips were incubated with a mouse monoclonal anti–β-tubulin antibody (clone 2-28-33; 1 μg/mL; Sigma) in blocking solution at a dilution of 1:2,000. After washing in 1× HBSS, goat anti-mouse immunoglobulin G (H + L) conjugated with Alexa Fluor 488 (1 μg/mL; Molecular Probes) was added in blocking solution to a final concentration of 2 μg/mL, which also contained Hoechst 33342 (2 μg/mL). Immunofluorescence was analyzed on the Everest Digital Microscopy Workstation (Intelligent Imaging Innovations).

Terminal deoxyribonucleotidyl transferase–mediated dUTP nick end labeling assay. Cells were treated with 5 nmol/L MPI-0441138 for 72 h and fragmented DNA was assessed by using the terminal deoxyribonucleotidyl transferase–mediated dUTP nick end labeling (TUNEL) assay. In the TUNEL assay, cells were fixed in 1% paraformaldehyde, washed in PBS, and then permeabilized with 70% ethanol (ApoBrdU TUNEL Assay Kit, Molecular Probes Europe BV). Labeling reactions using Alexa Fluor 488 dye–labeled anti-bromodeoxyuridine antibodies were done according to the manufacturer's protocol (Invitrogen). The fluorescein-labeled cells were analyzed by flow cytometry (FACScan, Becton Dickinson).

Apoptosis inducible factor and cytochrome *c* translocation. Cells were treated with 5 nmol/L MPI-0441138 or vehicle for 1 h and then fixed for 15 min with 4% paraformaldehyde in PBS. Cells were washed with PBS and permeabilized for 15 min with 0.1% saponin in PBS containing 1% bovine serum albumin and 0.1% sodium azide. Cells were incubated at room temperature for 1 h with either rabbit anti–cytochrome *c* antibody or rabbit anti–apoptosis inducible factor (AIF; Cell Signaling Technology, Inc.) at a concentration of 5.0 μg/mL, washed twice, and then incubated with anti-rabbit immunoglobulin/FITC swine $F(ab')_2$ secondary antibody (DakoCytomation GmbH) for 30 min. All incubations were done at room temperature. After washing, cells were analyzed by fluorescence microscopy (Olympus IX71, Olympus Optical GmbH) using a blue filter of 470 to 490 nm.

Measurement of mitochondrial membrane potential. Mitochondrial membrane potential ($\Delta\Psi_m$) was determined by staining of the cells with 5,5′,6,6′-tetrachloro-1,1′,3,3′-tetraethyl-benzimidazolylcarbicyanin iodide (JC-1). 22Rv1, MDA-MB-231, Caco-2, and Du145 cells were treated with 5 nmol/L MPI-0441138 for 12, 24, 48, or 72 h at 37°C. Cells were then incubated with BD MitoSensor reagent following the manufacturer's recommended conditions (JC-1, BD Biosciences). From each sample, 25,000 events were collected to measure fluorescence in the FL-2 channel after suitable compensation.

MDR testing. Exponentially growing MCF-7, NCI/ADR-RES, MCF-7/MX, MCF-7/VP, P388, and P388/ADR cells were seeded at 5,000 per well in a 96-well flat-bottomed microtiter plate and, 24 h later, culture medium was replaced with fresh medium and varying concentrations of test compound. Cellular viability was determined 72 h after addition of test compound by measuring intracellular ATP with the ATPLite assay system (Perkin-Elmer). All compounds were tested in quadruplicate. The effect of compounds on cell viability was calculated by comparing the ATP levels of cells exposed to test compound with those of cells exposed to vehicle. A semi-log plot of

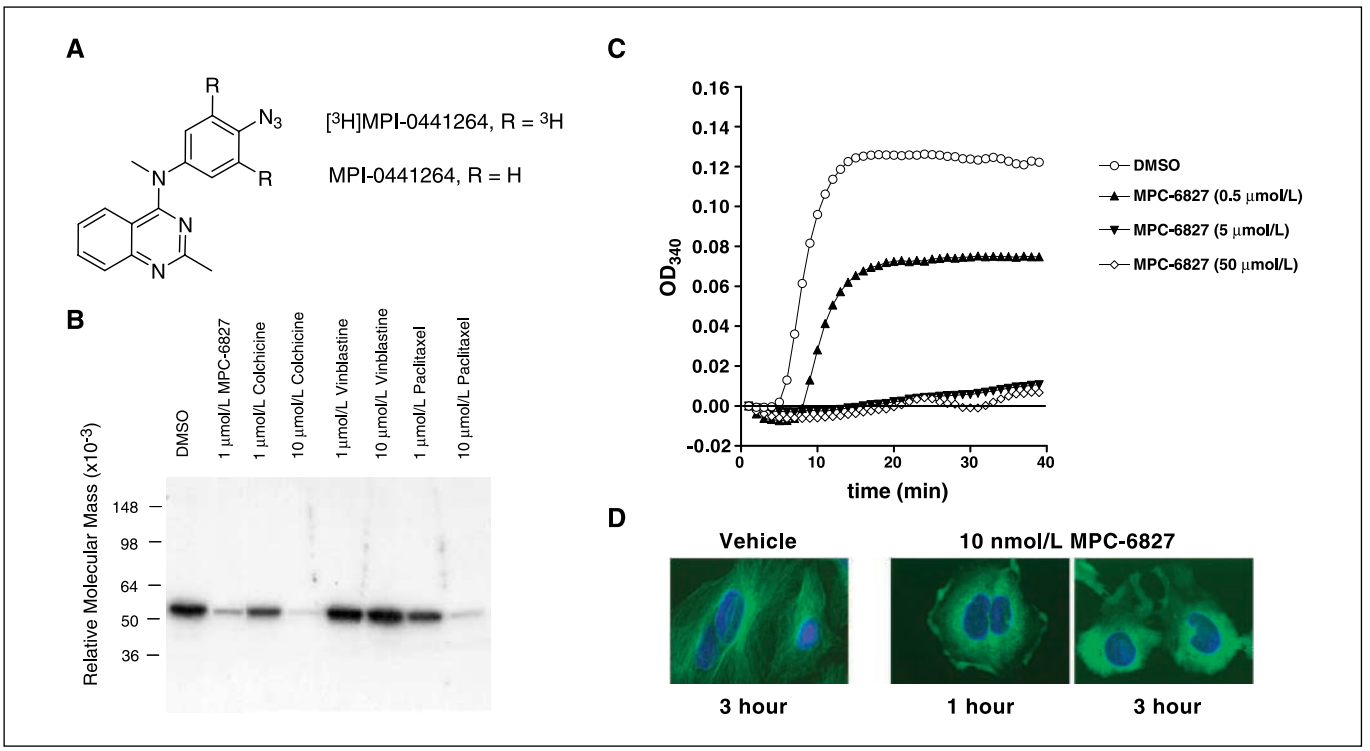

Figure 2. Tubulin is a cellular target of MPC-6827. *A,* structures of MPI-0441264 and [^{3}H]MPI-0441264. *B,* MPC-6827, colchicine, and paclitaxel, but not vinblastine, inhibit binding of a radioactive photoaffinity labeling analogue of MPC-6827 ([^{3}H]MPI-0441264) to a 55-kDa protein in Jurkat cells. *C,* MPC-6827 directly inhibits the polymerization of tubulin *in vitro*. *D,* MPC-6827 disrupts tubulin polymerization in human A549 lung cells. Coverslips containing A549 cells were incubated with vehicle or MPC-6827 (10 nmol/L) for 1 or 3 h. Coverslips were then stained with anti–β-tubulin antibody and Hoechst 33342.

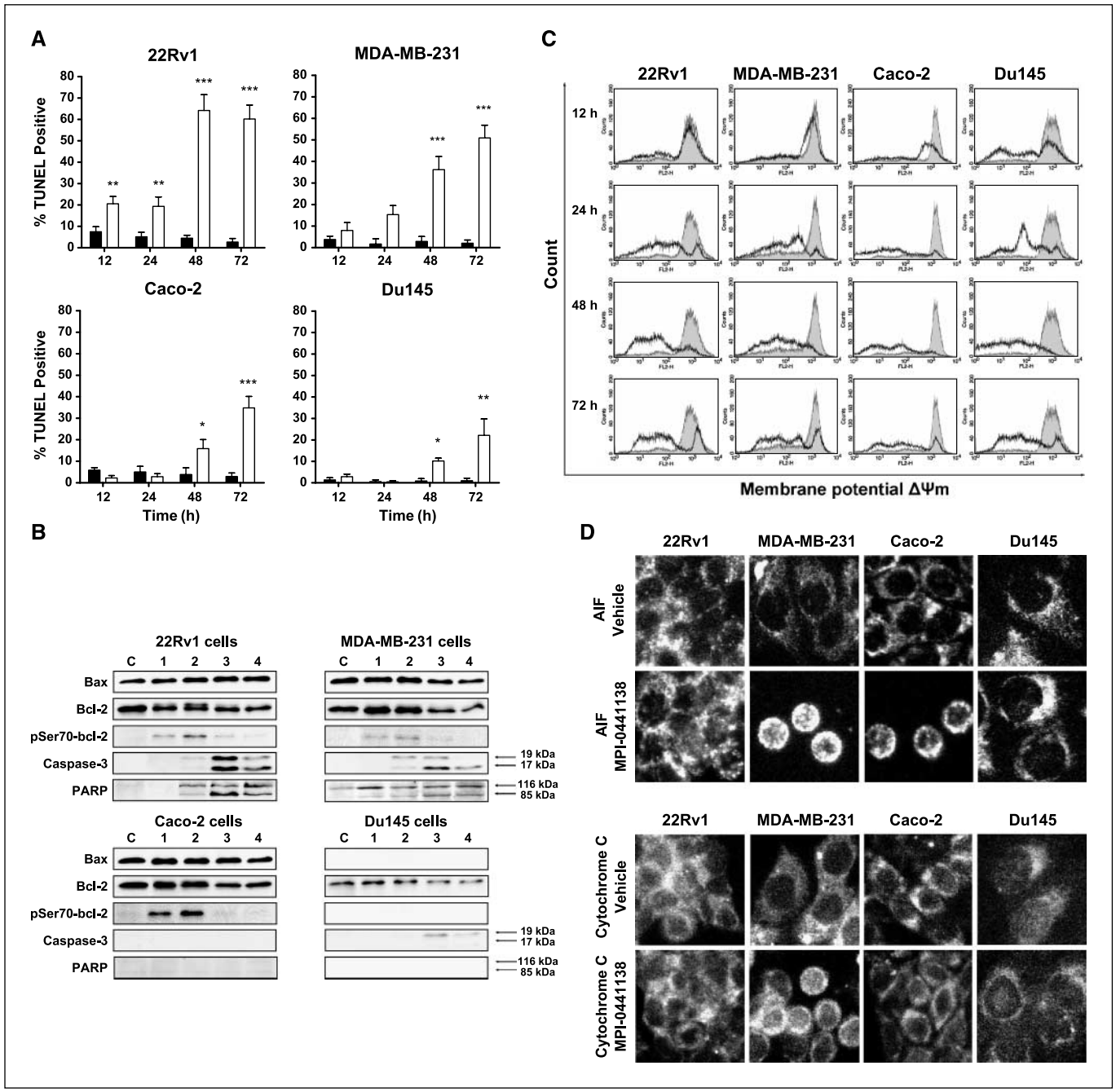

Figure 3. Participation of mitochondria in MPI-0441138–induced apoptosis. *A,* MPI-0441138 induces DNA fragmentation in 22Rv1, MDA-MB-231, Caco-2, and Du145 cells. Cells were treated with MPI-0441138 (5 nmol/L) and then incubated for 72 h. Control samples were allowed to grow in complete appropriate medium alone. Cells were analyzed for detection of single-strand DNA fragmentation by TUNEL assay. The percentage of TUNEL-positive cells was determined by quantifying the TUNEL-positive cells by fluorescence-activated cell sorting analysis. *Columns,* mean obtained from three independent experiments; *bars,* SD. *, $P < 0.05$; **, $P < 0.01$; ***, $P < 0.001$, versus vehicle-treated control. *B,* MPI-0441138 induces apoptosis-related protein expression. MPI-0441138–treated and untreated cells were subjected to Western blot analysis to investigate the expression of apoptosis-related proteins. Untreated cells were used as control. *Lanes 1* to *4,* MPI-0441138 (5 nmol/L) at 12, 24, 48, and 72 h, respectively. *C,* MPI-0441138 alters the membrane potential ($\Delta\Psi_m$) of mitochondria in 22Rv1, MDA-MB-231, Caco-2, and Du145 cells. Cells were treated with MPI-0441138 (5 nmol/L) and then incubated for 12, 24, 48, or 72 h. *Thin solid line with filled histogram,* mitochondrial membrane potential in the control untreated cells; *bold solid line,* $\Delta\Psi_m$ in MPI-0441138–treated cells. *D,* translocation of AIF and cytochrome *c* in MPI-0441138–treated cancer cells. Cells were treated with MPI-0441138 (5 nmol/L) for 1 h, fixed, and incubated with anti-AIF or anti–cytochrome *c* antibodies. Representative of three experiments.

relative ATP levels versus compound concentration was used to calculate the IC_{50}. Data were analyzed by Prism software by fitting it to a sigmoidal dose-response curve. The IC_{50} values obtained for individual data sets were combined to obtain mean IC_{50} and SD of the mean.

Mouse allografts and xenografts. For the B16-F1 allografts (1×10^6 cells per mouse) and the OVCAR-3 (10×10^6 cells per mouse), HT-29 (5×10^6 cells per mouse), MCF-7 (5×10^6 cells per mouse), and MDA-MB-231 (3×10^6 cells per mouse) xenografts, female Crl:Nu/Nu-nuBR mice (Charles River Labs) were implanted s.c. in the right flank with the indicated number of cells suspended in 100-μL HBSS or with Matrigel basement membrane (MDA-MB-231, BD Biosciences). For the MCF-7 xenografts, mice were implanted s.c. with 0.72 mg of 60-day time-release estradiol pellet

(Innovative Research of America) 48 h before the injection of cells. MX-1 tumors were passaged serially in CD1 nu/nu mice. For this study, tumors from several animals were excised. The viable portion of the tumor was cut into pieces ($\sim$30 mm^3) and implanted into the right lateral mammary pad of each animal using a trocar. In all the allografts and xenografts, tumors were allowed to grow to $\sim$100 mm^3 and then were placed into test groups (N = 10). The dose, route of administration, and dosing regimen for each study are indicated in Table 2. The mice were observed daily for mortality and signs of toxicity. Tumors and body weights were measured from day 1 to the end of study with the frequency measurements determined by the rate of growth of the tumor. Tumor growth was monitored using external measurements with a caliper and tumor volumes were calculated using the formula $\pi/6$ (width^2 $\times$ length), where width represents the smaller tumor diameter. Statistical ANOVA with unadjusted pairwise comparison was done using SAS software. These studies conformed to the recommendations set forth in the USPHS Policy on Humane Care and Use of Laboratory Animals (22).

Results and Discussion

MPC-6827 is a potent activator of caspases in various tumor cell lines. A novel series of 4-arylaminoquinazolines were identified as potent activators of caspases in a cell-based screening assay. The initial hit compound was identified in high-throughput screening by measuring the induction of apoptosis in T47D breast cancer cells using a profluorescent substrate (21). MPI-0441138 and MPC-6827 analogues (Fig. 1*A*) of the original screening hit showed activities in the low nanomolar range in the caspase activation assay (1.4 $\pm$ 0.3 and 2.5 $\pm$ 0.4 nmol/L, respectively). To investigate the rate and potency of cell killing, Jurkat cells were exposed to varying concentrations of MPC-6827 for 3 or 18 h. Although either 3 or 18 h of exposure showed equivalent maximal induction of cell death, MPC-6827 was apparently more potent after the longer length of exposure (Fig. 1*B*). To confirm that caspase activation was required for the MPC-6827–mediated induction of cell death, we tested the effect of MX-1013 (benzyloxycarbonyl-Val-Asp-fluoromethylketone), a pan-caspase inhibitor previously described to inhibit caspase activation (23). In the presence of both MPC-6827 and MX-1013, cell death of Jurkat cells was 11% as compared with 68% cell death in the presence of MPC-6827 alone (Fig. 1*C*). Furthermore, with the addition of MX-1013, the majority of MPC-6827–treated Jurkat cells were now arrested in G_2-M (Fig. 1*C*), indicating that the cells treated with MPC-6827 underwent G_2-M arrest before caspase activation and cell death. Taken together, these results support an apoptotic mechanism of cell killing by MPC-6827.

MPC-6827 competes with a radiolabeled and photoreactive analogue for binding to a 55-kDa protein. An azido photoaffinity analogue of MPC-6827, MPI-0441264, was synthesized, which remained potent in the caspase activation assay (data not shown). A tritiated version was also prepared and used to identify the molecular target of MPC-6827 ([^{3}H]MPI-0441264; Fig. 2*A*). Autoradiography of electrophoresed lysates from Jurkat cells treated with [^{3}H]MPI-0441264 revealed a prominent band at an apparent molecular weight of 55 kDa (Fig. 2*B*). To assess the specificity of the labeling by the affinity probe, Jurkat cells were pretreated with 1 μmol/L MPC-6827 before incubation with [^{3}H]MPI-0441264 and photoactivation. MPC-6827 significantly reduced the amount of photolabeled 55-kDa protein (Fig. 2*B*). Similar results were obtained with two additional azido photoaffinity analogues of MPC-6827 in which the azido group was located at different positions on the molecule (not shown).

Due to the apparent molecular weight of the bound protein and the cell cycle profile of the compound treated cells, the 55-kDa bound protein was suspected to be tubulin. Therefore, compounds known to bind tubulin, such as colchicine, paclitaxel, and vinblastine, were tested for the ability to compete with the [^{3}H]MPI-0441264 labeling. As shown in Fig. 2*B*, the 55-kDa labeled protein was clearly competed by MPC-6827, colchicine, and paclitaxel, but not by vinblastine, suggesting the 55-kDa band was likely tubulin.

MPC-6827 disrupts tubulin polymerization *in vitro*, binds to the colchicine-binding site, and disrupts microtubules in intact cells. To confirm that MPC-6827 bound tubulin and altered polymerization, we evaluated its effect on tubulin polymerization in an *in vitro* assay. MPC-6827 was tested at 0.5, 5, and 50 μmol/L, and 5 μmol/L was sufficient to completely inhibit tubulin polymerization (Fig. 2*C*). Although this potency for inhibition of tubulin polymerization seemed to be low, it is likely not inconsistent with cellular potency for apoptosis induction, considering the high concentration of tubulin in the polymerization assay.

The *in vitro* studies clearly showed that MPC-6827 binds to tubulin and disrupts microtubule formation. We also wanted to determine if MPC-6827 was able to inhibit microtubule formation in intact cells. Microtubule disruption was rapidly induced in human A549 non–small-cell lung carcinoma cells, treated with vehicle or 10 nmol/L MPC-6827, with marked disruption after 1 h and complete disruption by 3 h (Fig. 2*D*). This microtubule disruption activity is most consistent with MPC-6827 exerting functional effects through the colchicine rather than the taxane binding site on tubulin because colchicine is known to inhibit and taxanes are known to stabilize tubulin polymerization (9). Rather than direct competition, the ability of paclitaxel to prevent labeling of the 55-kDa protein in the cellular assay may be due to microtubule stabilization from paclitaxel treatment that can block MPC-6827 from binding to the colchicine site.

MPI-0441138–induced cell death shows multiple hallmarks of apoptosis. MPI-0441138 is a close analogue of MPC-6827 and shows similar caspase activation potency. To determine whether

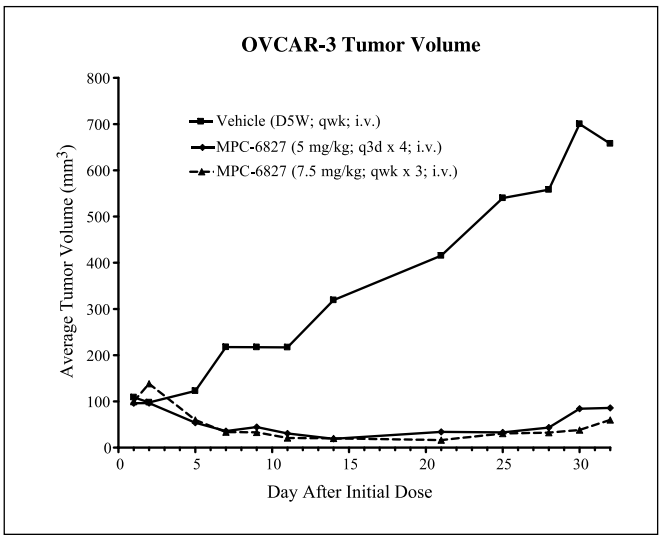

Figure 4. MPC-6827 inhibits the growth of established OVCAR-3 tumor xenografts in athymic nude mice. OVCAR-3 tumors were established in athymic nude mice. I.v. dosing of MPC-6827 was delivered either at 5 mg/kg on days 1, 4, and 7 or at 7.5 mg/kg on days 1, 8, and 15 when the average tumor volume reached 100 mm^3. Representative of two experiments.

MPI-0441138 induced apoptosis in tumor cells, a variety of markers of apoptosis were evaluated in prostate carcinoma Du145 and 22Rv1 cells, colorectal carcinoma Caco-2 cells, or breast carcinoma MDA-MB-231 cells. MPI-0441138 induced DNA fragmentation in all of the tumor cell lines investigated, with the most prominent responses observed in 22Rv1 and MDA-MB-231 cells (61 ± 6.5% and 51 ± 6.0%, respectively; Fig. 3*A*). Induction of DNA fragmentation in 22Rv1 and MDA-MB-231 cells was accompanied by robust caspase-3 activation and poly(ADP-ribose) polymerase cleavage (Fig. 3*B*). Changes in mitochondrial membrane potential ($\Delta\Psi_m$) in the treated cancer cells were also assessed, with MPI-0441138 significantly altering $\Delta\Psi_m$ in all cancer cells after 24 h. The most prominent $\Delta\Psi_m$ dissipation was observed in 22Rv1, MDA-MB-231, and Caco-2 cells with a loss of 69%, 66%, and 79%, respectively. Du145 cells revealed the lowest dissipation of the $\Delta\Psi_m$ after 24 h (47%), but this effect increased to 78% after 48 h (Fig. 3*C*). The effect of MPI-0441138 on AIF and cytochrome *c* translocation from mitochondria to cytosol and nucleus was assessed by immunofluorescence microscopy. The most active translocation of AIF was observed in MDA-MB-231 and Caco-2 cells. The most active translocation of AIF was observed in MDA-MB-231 and Caco-2 cells. MDA-MB-231 cells also revealed translocation of cytochrome *c* from mitochondria to nucleus. 22Rv1 and Du145 cells showed slightly lagging AIF and cytochrome *c* translocation on MPC-6827 treatment (Fig. 3*D*). The microscopic analysis of translocation of AIF and cytochrome *c* was confirmed by cellular fractionation and Western blot analysis (data not shown). Collectively, these results show that MPI-0441138, and therefore MPC-6827 by analogy, induces cell death through a mechanism consistent with activation of the intrinsic apoptotic pathway.

MPC-6827 is effective in MDR cancer cell lines *in vitro*. Human breast carcinoma NCI/ADR-RES (previously called MCF-7/ADR) and human leukemia P388-ADR cell lines overexpressing MDR-1 (Pgp-1) were tested for resistance to MPC-6827 and the tubulin-interacting chemotherapeutics vinblastine and docetaxel. MPC-6827 showed similar growth inhibition against P388 and P388/ADR with an IC_{50} of 1.5 nmol/L. MPC-6827 inhibited the growth rate of MCF-7 and NCI/ADR-RES cells, with IC_{50} values of 2.1 and 1.5 nmol/L, respectively. Vinblastine was much less active against the MDR-1–overexpressing cells with IC_{50} values of 186 and 551 nmol/L for P388/ADR and NCI/ADR-RES cells, respectively, as compared with 1.5 and 0.6 nmol/L for P388 and MCF-7 cells. Docetaxel was also less active in the MDR-1–overexpressing cells with IC_{50} values of 83 and 340 nmol/L for P388/ADR and NCI/ADR-RES cells, respectively, versus 6.8 and 1.4 nmol/L for P388 and MCF-7 cells (Table 1). MPC-6827 also showed similar growth inhibition in MCF-7 and the BCRP-1–overexpressing cell lines. Irinotecan and epirubicin, which are substrates of the BCRP-1 pump (24), were less active against the BCRP-1–overexpressing cell line MCF-7/MX with IC_{50} values of 220 and 1,500 nmol/L, as opposed to 16 and 50 nmol/L for MCF-7 cells, respectively. MPC-6827 showed similar cytotoxic activity against MCF-7 and the MRP-1–overexpressing cell line MCF-7/VP, with IC_{50} values of 2.1 and 1.3 nmol/L for MCF-7 and MCF-7/VP cells, respectively. Epirubicin, a substrate of the MRP-1 pump (25), was less active against MCF-7/VP cells with an IC_{50} of 960 nmol/L as compared with 150 nmol/L for MCF-7 cells. These results show that MPC-6827 is not a substrate for the MDR transporters Pgp-1, BCRP-1, and MRP-1 in human cancer cell lines *in vitro*.

MPC-6827 inhibits tumor growth *in vivo*. The *in vivo* efficacy of MPC-6827 was studied in s.c. allograft and xenograft models using mouse B16 melanoma and human breast (MCF-7, MX-1, and MB-MDA-435), colon (HT-29), pancreas (MIAPaCa-2), and ovarian (OVCAR-3) tumor cell lines. After implantation into the right flank region of athymic nude mice, tumors were allowed to grow to an average volume of 100 mm^3 before beginning treatment with MPC-6827. The results of each of the allograft and xenograft studies are summarized in Table 2 and an example result from a xenograft study is shown in Fig. 4. These data indicate that MPC-6827 was efficacious in inhibiting the growth of a broad panel of tumor types.

These studies show that MPC-6827 acts through binding the colchicine site on β-tubulin, inhibiting tubulin polymerization and leading to G_2-M arrest and apoptosis, which is activated through the intrinsic mitochondrial pathway. MPC-6827 also showed efficacy *in vitro* against tumor cells overexpressing the three main ABC transporters responsible for MDR, and, therefore, MPC-6827 may prove effective against drug-resistant tumors in the clinic. Importantly, MPC-6827 displayed significant inhibition of the growth of a broad spectrum of solid tumor types in xenograft models.

Currently, the macrolide epothilones are the most advanced new tubulin targeting agents in the clinic (26). Epothilones are chemically distinct from taxanes but bind to the same binding

Table 1. Cytotoxicity of MPC-6827 in non–drug-resistant cells and in cells expressing ABC MDR transporters

Cell line (ABC transporter)	IC_{50} (nmol/L)				
	MPC-6827	Epirubicin	Vinblastine	Docetaxel	Irinotecan
P388	1.5 ± 0.2	ND	1.5 ± 0.2	6.8 ± 3	ND
P388/ADR (MDR-1)	1.5 ± 0.3	ND	190 ± 51	83 + 40	ND
MCF-7	2.1 ± 0.2	150 ± 43	0.6 ± 0.1	1.4 ± 0.9	16 ± 1.4
NCI/ADR-RES (MDR-1)	1.5 ± 0.1	ND	551 ± 91	340 + 59	ND
MCF-7/MX (BCRP-1)	3.4 ± 0.7	1,500 ± 730	ND	ND	220 ± 35
MCF-7/VP (MRP-1)	1.3 ± 0.3	960 ± 110	ND	ND	ND

NOTE: MPC-6827 is not a substrate for ABC transporters. Determination of the cytotoxicity of MPC-6827 in normal expressing cells and cells overexpressing the MDR transporters MDR-1, MCP-1, and BCRP-1. NCI/ADR-RES and P388/ADR, MCF-7/MX, and MCF-7/VP overexpress MDR-1 (Pgp-1), BCRP-1, and MRP-1, respectively. Data are given as average and SD of three independent experiments. ND, not determined.

Table 2. Activity of i.v. administered MPC-6827 in female Crl:Nu/Nu mouse xenograft models

Xenograft model	Dose of MPC-6827 (mg/kg)	Dosing regimen	% Tumor growth inhibition	*P*
B16-F1	2.5	q1w × 2	51 (d11)	0.0017
	5	q1w × 2	67 (d11)	<0.0001
OVCAR-3	5	q3d × 4	88 (d32)	0.0028
	7.5	q1w × 3	95 (d32)	0.0001
HT-29	5	q1w × 3	29 (d22)	0.037
MIA PaCa	5	q1w × 3	49 (d18)	0.02
MCF-7	5	q1w × 3	53 (d22)	0.003
	10	q1w × 3	71 (d22)	0.0006
MX-1	2.5	q1w × 3	70 (d27)	0.02
	5.0	q1w × 3	96 (d27)	0.002
MDA MB-435	2.5	q1w × 7	58 (d54)	0.08
	5.0	q1w × 7	71 (d54)	0.04

NOTE: MPC-6827 treatment significantly inhibits the growth of established tumor allografts and xenografts in athymic mice. The indicated tumors were established as s.c. allografts or xenografts in athymic nude mice. Treatment with i.v. MPC-6827 was initiated on the day the average tumor volume achieved 100 mm^3 (N = 10). The subsequent maximal tumor growth inhibition values are listed with the day the measurement was made post-initial dose in parentheses.

region on β-tubulin and exert their biological effects by stabilizing microtubules. The potential advantages of the epothilones over the taxanes are better aqueous solubility, greatly reduced affinity toward drug resistance–mediating ABC transporters, and significant activity against taxane-resistant tumor cells (27, 28). MPC-6827 is unique from the epothilones in that it binds to the colchicine site on β-tubulin and is an inhibitor of microtubule formation. Although MPC-6827 is equally potent in cell lines regardless of ABC transporter expression, its activity in xenograft models using taxane-resistant tumor cells has yet to be determined.

MPC-6827 has recently opened a phase II clinical trial designed to determine the safety profile and the extent of its ability to improve the survival of patients with glioblastoma multiforme and melanoma that has spread to the brain.

Acknowledgments

Received 1/11/2007; revised 3/28/2007; accepted 4/20/2007.

The costs of publication of this article were defrayed in part by the payment of page charges. This article must therefore be hereby marked *advertisement* in accordance with 18 U.S.C. Section 1734 solely to indicate this fact.

References

1. Herr I, Debatin K. Cellular stress response and apoptosis in cancer therapy. Blood 2001;98:2603–14.
2. Kasibhatla S, Tseng B. Why target apoptosis in cancer treatment? Mol Cancer Ther 2003;2:573–80.
3. Rich T, Allen R, Wyllie A. Defying death after DNA damage. Nature 2000;407:777–83.
4. Degterev A, Boyce M, Yaun J. A decade of caspases. Oncogene 2003;22:8543–67.
5. Lavrik IN, Golks A, Krammer PH. Caspases: pharmacological manipulation of cell death. J Clin Invest 2005;115:2665–72.
6. Strasser A, O'Conner L, Dixit VM. Apoptosis signaling. Annu Rev Biochem 2000;69:217–45.
7. Locksley RM, Killeen N, Lenardo MJ. The TNF and TNF receptor superfamilies: integrating mammalian biology. Cell 2001;104:487–501.
8. Desagher S, Martinou J. Mitochondria as the central control point of apoptosis. Trends Cell Biol 2000;10:369–77.
9. Green DR, Reed JC. Mitochondria and apoptosis. Science 1999;309:312.
10. Huang Z. Bcl-2 family proteins as targets for anticancer drug design. Oncogene 1999;19:6627–31.
11. Jordan MA, Wilson L. Microtubules as a target for anticancer drugs. Nat Rev Cancer 2004;4:253–65.
12. Zhou J, Giannakakou P. Targeting microtubules for cancer chemotherapy. Curr Med Chem Anti-Canc Agents 2005;5:65–71.
13. Dumontet C, Sikic BI. Mechansims of action and resistance to antitubulin agents: microtubule dynamics, drug transport and cell death. J Clin Oncol 1999;17:1061–70.
14. Leonard GD, Fojo T, Bates SE. The role of ABC transporters in clinical practice. Oncologist 2003;8:411–24.
15. Fojo AT, Menefee M. Microtubule targeting agents: basic mechanisms of multidrug resistance (MDR). Semin Oncol 2005;32:S3–8.
16. Miglarese MR, Carlson RO. Development of new cancer therapeutic agents targeting mitosis. Expert Opin Investig Drugs 2006;15:1411–25.
17. Kuppens I. Current State of the Art of new tubulin inhibitors in the clinic. Curr Clin Pharm 2006;1:57–70.
18. Pirnia F, Breuleux M, Schneider E, et al. Uncertain identity of doxorubicin-resistant MCF-7 cell lines expressing mutated p53. J Natl Cancer Inst 2000;92:1535–6.
19. Chitnis MP, Johnson RK. Biochemical parameters of resistance of an Adriamycin-resistant subline of P388 leukemia to emetine, an inhibitor of protein synthesis. J Natl Cancer Inst 1978;60:1049–54.
20. Taylor CW, Dalton WS, Parrish PR, et al. Different mechanisms of decreased drug accumulation in doxorubicin and mitoxantrone resistant variants of the MCF7 human breast cancer cell line. Br J Cancer 1991;63:923–9.
21. Cai SX, Zhang HS, Guastella J, et al. Design and synthesis of rhodamine 110 derivative and caspase-3 substrate for enzyme and cell-based fluorescent assay. Bioorg Med Chem Lett 2001;11:39–42.
22. The U.S. Public Health Service Policy on Humane Care and Use of Laboratory Animals, available from the Office of Laboratory Animal Welfare, National Institutes of Health, Department of Health and Human Services, RKLI, Suite 360, MSC 7982, 6705 Rockledge Drive, Bethesda, MD 20892-7982.
23. Yang W, Guastella J, Huang JC, et al. MX1013, a dipeptide caspase inhibitor with potent *in vivo* anti-apoptotic activity. Br J Pharmacol 2003;140:402–12.
24. Nakagawa M, Schneider E, Dixon KH, et al. Reduced intracellular drug accumulation in the absence of P-glycoprotein (MDR1) overexpression in mitoxantrone-resistant human MCF-7 breast cancer cells. Cancer Res 1992;52:6175–81.
25. Schneider E, Horton JK, Yang CH, et al. Multidrug resistance-associated protein gene overexpression and reduced drug sensitivity of topoisomerase II in a human breast carcinoma MCF7 cell line selected for etoposide resistance. Cancer Res 1994;54:152–8.
26. Larkin JM, Kaye SB. Epothilones in the treatment of cancer. Expert Opin Investig Drugs 2006;15:691–702.
27. Chou T, Zhang X, Harris CR, et al. Desoxyepothilone B is curative against human tumors xenografts that are refractory to paclitaxel. Proc Natl Acad Sci U S A 1998;95:15798–802.
28. Lee FY, Borzilleri R, Fairchild CR, et al. BMS-247550: a novel epothilone with a mode of action similar to paclitaxel but possessing superior antitumor activity. Clin Cancer Res 2001;7:1429–37.

MPC-6827: A Small-Molecule Inhibitor of Microtubule Formation That Is Not a Substrate for Multidrug Resistance Pumps

Shailaja Kasibhatla, Vijay Baichwal, Sui Xiong Cai, et al.

Cancer Res 2007;67:5865-5871.